Computational Exploration of *Berberis lycium* Royle: A Hidden Treasure Trove for Antiviral Development

Bioinformatics and Biology Insights
Volume 18: 1–19

DOI: 10.1177/11779322241264144

Mamuna Mukhtar[1], Haris Ahmed Khan[1,2], Tope Abraham Ibisanmi[3], Ayodele Ifeoluwa Faleti[4] and Najam us Sahar Sadaf Zaidi[1,5]

[1]Department of Industrial Biotechnology, Atta ur Rahman School of Applied Biosciences, National University of Sciences and Technology, Islamabad, Pakistan. [2]Department of Biotechnology, University of Mianwali, Mianwali, Pakistan. [3]Department of Microbiology, School of Life Sciences, The Federal University of Technology Akure, Akure, Nigeria. [4]Department of Chemistry, School of Physical Sciences, The Federal University of Technology Akure, Akure, Nigeria. [5]Department of Biological and Health Sciences, Pak-Austria Fachhochschule: Institute of Applied Sciences and Technology, Mang, Haripur-KPK, Pakistan.

ABSTRACT: Viral infections and associated illnesses account for approximately 3.5 million global fatalities and public health problems. Medicinal plants, with their wide therapeutic range and minimal side effects, have gained limelight particularly in response to growing concerns about drug resistance and sluggish development of antiviral drugs. This study computationally assessed 11 chemical compounds from *Berberis lycium* along with two antiviral drugs to inhibit SARS CoV 2 (coronavirus disease 2019 [COVID-19]) RNA-dependent RNA polymerase (RdRP), influenza virus RdRP, and two crucial dengue virus (DENV) enzymes (NS2B/NS3 protease and NS5 polymerase). Berberine and oxyberberine passed all pharmacokinetics analysis filters including Lipinski rule, blood-brain barrier permeant, and cytochrome suppression and demonstrated drug-likeness, bioavailability, and a non-toxic profile. Docking of phytochemicals from *B lycium* returned promising results with selected viral proteins, ie, DENV NS2BNS3 (punjabine –10.9 kcal/mol), DENV NS5 (punjabine –10.4 kcal/mol), COVID-19 RdRP (oxyacanthine –9.5 kcal/mol), and influenza RdRP (punjabine –10.4 kcal/mol). The optimal pharmacokinetics of berberine exhibited good binding energies with NS2BNS3 (–8.0 kcal/mol), NS5 (–8.3 kcal/mol), COVID RdRP (–7.7 kcal/mol), and influenza RdRP (–8.3 kcal/mol), while molecular dynamics simulation of a 50-ns time scale by GROMACS software package provided insights into the flexibility and stability of the complexes. A hidden treasure trove for antiviral research, berberine, berbamine, berbamunine, oxyberberine, oxyacanthine, baluchistanamine, and sindamine has showed encouraging findings as possible lead compounds. Pharmacological analyses provide credence for the proposed study; nevertheless, as the antiviral mechanisms of action of these phytochemicals are not well understood, additional research and clinical trials are required to demonstrate both their efficacy and toxicity through in vitro and in vivo studies.

KEYWORDS: Medicinal plants, *Berberis lycium*, pharmacokinetics, MD simulation, viral infections

RECEIVED: November 5, 2023. **ACCEPTED:** June 6, 2024.

TYPE: Research Article

FUNDING: The author(s) received no financial support for the research, authorship, and/or publication of this article.

DECLARATION OF CONFLICTING INTERESTS: The author(s) declared no potential conflicts of interest with respect to the research, authorship, and/or publication of this article.

CORRESPONDING AUTHOR: Najam us Sahar Sadaf Zaidi, Atta ur Rahman School of Applied Biosciences, National University of Sciences and Technology, Sector H-12, Islamabad, Pakistan; Department of Biological and Health Sciences, Pak-Austria Fachhochschule: Institute of Applied Sciences and Technology, Mang, Khanpur Road, Haripur-KPK, 22650, Pakistan. Email: Sadafzaidi@asab.nust.edu.pk

Introduction

Throughout history, viral epidemics and pandemic illnesses have posed serious threats to humanity and had far-reaching consequences for civilization. There are more than 220 viral species that may infect people, and 80% of them are tenacious in animals on their own.[1] Viruses are recognized for the dangerous contagious diseases they induce, such as HIV, hepatitis B virus and hepatitis C virus (HCV), coronaviruses such as Middle Eastern respiratory syndrome and severe acute respiratory syndrome coronavirus 2 (SARS-CoV-2), Zika virus, Nipah virus, smallpox, influenza, Ebola virus, Dengue virus (DENV), and Chikungunya virus.[2-4] A sizable portion of deaths worldwide and public health issues are caused by viral infections and related disorders. Globally, infectious illnesses claim the lives of 3.5 million individuals every year. The major health risk to people in their lives is the current coronavirus disease 2019 (COVID-19) epidemic.[5] SARS-CoV-2, a member of the Betacoronavirus family of enveloped single-strand RNA viruses in the Coronaviridae, was initially discovered in China in late 2019. Since then, it has spread over the world, causing the COVID-19 epidemic, which as of the beginning of April 2021 had killed over 2.84 million people and afflicted more than 130 million others.[6,7] The influenza A virus can cause serious respiratory conditions or other health issues in people and has a high rate of infectiousness and dissemination among many animals.[8] Approximately, one-third of the global population, who reside in tropical and subtropical areas, is seriously at risk of getting dengue fever. Dengue fever infections have also dramatically increased during the past few decades. The World Health Organization estimates that 390 million new dengue fever infections occur each year worldwide.[9]

Different antiviral strategies have been employed against these viral pathogens. Favipiravir, also known as T-705, is an antiviral drug that was approved for use in Japan in 2014 to treat illnesses brought on by the pandemic influenza virus. The drug undergoes intracellular transformation into its active, phosphoribosylated state, which the viral RNA-dependent RNA polymerase (RdRP) recognizes as a substrate. It's amazing to learn that this substance, in addition to having anti-influenza virus behavior, can also prevent the replication of flavi, alpha, filo, bunya, arena, noro, and other RNA viruses, including neglected and (re)emerging viruses for which there is

currently no antiviral treatment available.[10,11] Remdesivir has demonstrated its efficacy against a number of other viral infections, especially SARS-CoV-2, for which it has recently acquired Food and Drug Administration approval after data demonstrating a shortened time to recovery in patients with hospitalized COVID-19.[12] There has been a significant breakthrough on the subject of herbal antiviral therapy because of rising concerns about the establishment of drug resistance and the sluggish progress in the development of antiviral medications. Medicinal plants have been used widely throughout history in almost all countries for the treatment of diseases and maladies as conventional medical therapies due to its wide therapeutic spectrum and few to no side effects. Every effort has been made to identify innovative pharmaceuticals and complementary/alternative therapies generated from diverse herbal preparations as the majority of viral infections cannot be treated with synthetic antiviral medications.[13]

Berberis lycium, a member of the genus Berberry of family Berberidaceae, is a thorny shrub. Berberry grows in many countries across the world and comprises 450 to 500 varieties of deciduous or evergreen bushes that are important both medicinally and economically. The species is found across Himalaya region of India and Pakistan, primarily in hilly areas of Azad Kashmir and Khyber Pakhtunkhwa province.[14-16] The plant has historically been used as a diuretic, cough suppressant, and diaphoretic as well as a treatment for fever, scabies, piles, jaundice, internal sores, rheumatism, diabetes, eye infections, respiratory illnesses, backache, and scabies. Anti-diabetic, hepatoprotective, antimicrobial, fungicidal, insecticidal, antimutagenic, and wound-healing characteristics are all present in the plant *B lycium*.[17-19] On this shrub, the blooms are visible from April through June. The British and Indian pharmacopeias both cite this plant's numerous therapeutic qualities. The berries, roots, and bark are all used to make remedies. Jaundice and wounds are two common conditions treated with this herb. The locals consume the succulent fruits of the plant uncooked or use them to make juices, marmalades, and other tasty treats. These fruits are an excellent source of antioxidants, anthocyanin, and other nutrients.[20,21] The natural yellow alkaloid berberine, which is mostly found in the roots of this plant, has a long history of usage in Native American and Chinese traditional medicine. Alkaloids, which are found in many commercially significant plant families, make up one of the biggest classes of secondary metabolites in plants. Alkaloids include neuroactive substances like caffeine and nicotine as well as lifesaving medications like the antitumoral vincristine and vinblastine and the medication emetine, which is used to combat oral intoxication. The metabolism and accumulation of alkaloids are studied using several approaches. Monitoring the concentration of the alkaloid, its precursors, and their enzyme activities under controlled assaults by pathogens and herbivores, or while simulating their presence by chemical or physical stimulation, is an effective method.[22] For more than 3000 years, Chinese and Ayurvedic medicine have employed this plant's extracts and decoctions.[23,24] In addition, studies using animal models have demonstrated the anticancer, antioxidant, antitumor, anti-urolithic, and wound-healing properties of fruit extract, stem bark, and root bark. Even if utilization and acceptance of medicinal plants have grown, toxicity evaluations and the scientific evidence for their traditional use continue to be major problems.[25]

Pharmaceutical drugs manufactured from local plants are particularly useful in many developing countries for the prevention and treatment of numerous human ailments due to their well-established properties. About 61% of innovative medications created in the late 20th and early 21st centuries for the effective treatment of cancer and infectious diseases were based on natural materials. Steroids, alkaloids, carotenoids, flavonoids, tannins, terpenoids, and glycosides are major bioactive compounds of plants that are used as a foundation for the development of pharmaceuticals.[26] Natural chemicals have a variety of pharmacological characteristics and have been reported to be potent antivirals. The global interest in developing an anti-viral medication from natural chemicals against viruses has intensified. The present effort is focused on direct-acting antivirals, which are medications that inhibit viral replication largely by attacking viral proteases and polymerases.[27,28] *B lycium* has extensively been studied for their antimicrobial,[24,29] antioxidant,[30] antidiabetic,[21] and wound-healing properties[31]; however, their antiviral potentials have remained unexplored till date. The objective of the present investigation was to evaluate the capacity of 11 compounds from *B lycium* and two pharmaceuticals to inhibit the RdRP of COVID-19, the RdRP of influenza virus, and two key DENV enzymes (NS2B/NS3 protease and NS5 polymerase). Numerous pharmacokinetic analyses showed the phytoligands' drug-likeness and toxicity potential for the assessment of suitable leads to develop an anti-dengue medication. These tests were used to evaluate the docked structures for ligand-protein complexes for stability. Several publications, including older research and literature concerning its folklore claims, have already emphasized the potential of this herb in medicine. This in turn provided rationale for the ongoing initiatives.

Materials and Methods

Retrieval of ligand and receptor proteins

For the research design, 11 bioactive constituents from *B lycium* were selected along with two standard antiviral drugs so that their physicochemical and pharmaceutical qualities could be compared to those of the chosen bioactive constituents.[18,32,33] The three-dimensional structures of the chosen compounds were retrieved in SDF version from PubChem and converted into PDB format using Biovia Discovery Studio. All ligands, ions, and water molecules were deleted from the PDB files to prepare the protein input file. Polar hydrogens were then

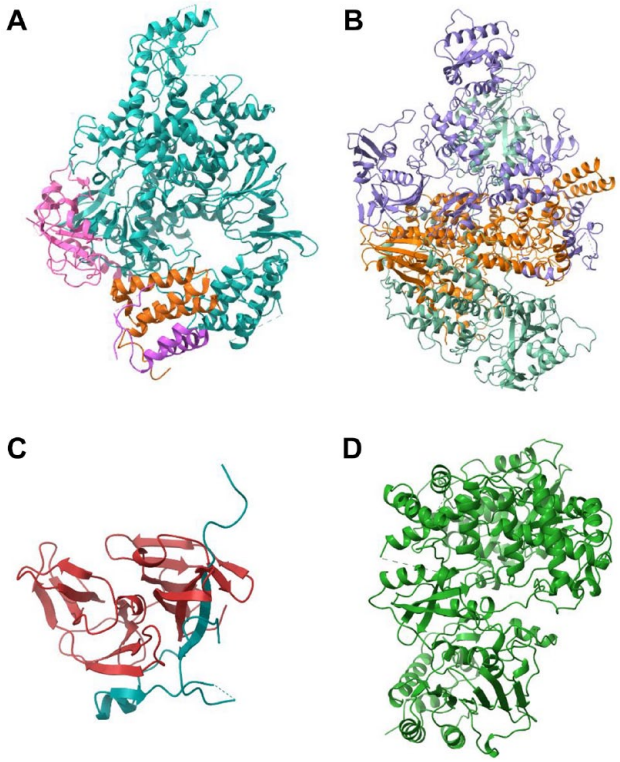

Figure 1. Visual representation of selected 3D crystal structures of (A) COVID-19 RdRP (PDB ID: 6M71), (B) influenza RdRP (PDB ID: 6QPF), (C) DENV NS2B/NS3 protease (PDB ID: 2FOM), and (D) DENV NS5 polymerase (PDB ID: 4V0Q) downloaded from PDB.
Abbreviations: PDB ID, Protein Data Bank identifier; RdRP, RNA-dependent RNA polymerase.

included, the partial atomic charge was estimated using the Kollman-united charge, and the resulting file was exported in PDBQT format to be utilized in the subsequent phases.[34]

The 3D crystal structures of COVID-19 RdRP (PDB ID: 6M71), influenza RdRP (PDB ID: 6QPF), and two DENV proteins, ie, NS2B/NS3 protease (PDB ID: 2FOM) and NS5 polymerase (PDB ID: 4V0Q), available in Research collaboratory for Structural Bioinformatics (RCSB) database, were downloaded from Protein Data Bank in PDB format. The 3D protein architectures (Figure 1) were improved before being subjected to docking studies. The chosen proteins were refined by removing unimportant ions, ligands (if there are any), and water molecules. In addition, the receptor proteins were given polar hydrogen atoms and Kollman charges before being stored in PDBQT format for docking.[35]

Pharmacokinetic absorption, distribution, metabolism, and excretion analysis

Swiss-ADME program was used to forecast the absorption, distribution, metabolism, and excretion (ADME) characteristics of all the studied plant metabolites. The program examines crucial pharmacokinetic characteristics of a substance such as blood-brain barrier (BBB), cytochrome P450 viz CYP1A2, CYP2C19, CYP2C9, CYP2D6, CYP3A4 inhibitor, metabolism as a P-glycoprotein (P-gp) substrate, lipophilicity for plasma membrane absorption, and gastrointestinal (GI) absorption.[36,37] The Lipinski rule of five, Ghose rule, Veber rule, Egan rule, and Muegge rule offer credible parameters that can be utilized as a rapid guide for evaluating the pharmacological effects and drug-likeness of new compounds that could have potential therapeutic applications. For the pharmaceutical to retain its bioavailability, there shouldn't be more than one Lipinski violation.[38-40] Lipinski rule of five states that hydrogen-bond donors should be less than 5, less than 10 hydrogen-bond acceptors, the molecular weight less than 500 Da (MW ⩽500), lipophilicity (LogP ⩽5) should be less than 5, and total polar surface area (TPSA) not more than 140 Å.[41] Ghose filter suggest 160 ⩽ MW ⩽ 480, −0.4 ⩽ WLogP (lipophilicity) ⩽ 5.6, 40 ⩽ the molar refractivity ⩽ 130, and 20 ⩽ number of atoms ⩽ 70.[42] Veber guidelines state that the active substance has a total hydrogen bond ⩽12, and rotatable bond number ⩽10. Oral bioavailability for polar surface area of ⩽140 tends to be about 20%.[43] Egan rule involves lipophilicity (WLogP) ⩽5.88 and the TPSA ⩽131.6.[44] Muegge rule states 200 ⩽ MW ⩽ 600, −2 ⩽ XLogP3 (lipophilicity) ⩽ 5, the TPSA ⩽150, the number of rings ⩽7, the number of carbons >4, the number of heteroatoms >1, the number of rotatable bonds ⩽15, the hydrogen-bond acceptors ⩽10, and the hydrogen-bond donors ⩽5.[45]

A satisfactory bioavailability is expected for molecules whose parameter values do not go above the upper bound. All the bioavailability parameter computations were done using the Molinspiration software v2022.08. The program forecasted how well the phytoconstituents would interact with human receptors (eg, G protein-coupled receptors [GPCRs], kinases, proteases, ion channels, enzymes, and nuclear receptors). If the bioactivity score >0.0, then the compound is active; moderately active if it is in the range between −5.0 and 0.0, and inactive if the bioactivity score is less than −5.0.[46,47]

Toxicity analysis

The toxicity and drug-likeness of the substances that were filtered by the ADME analysis were assessed by OSIRIS DataWarrior v5.2.1 software. A library of about 5300 substructure elements and the accompanying drug-likeness scores serve as the foundation for the computation. Through toxicity risk assessment, the impacts of drug toxicity, such as mutagenicity, irritation, tumorigenicity, and reproductive consequences, were investigated. Tumorigenesis is the process through which healthy cells turn into cancerous cells, which can subsequently multiply and divide uncontrollably to create a mass or tumor,[48] whereas the capacity of a material, agent, or procedure to cause cancer is referred to as being carcinogenic. This investigation provides preliminary data on possible adverse effects of phytocompounds that may be used in the discovery and development of new drugs.[49,50]

Table 1. Grid sizes and grid centers used in AutoDock Vina 1.5.6.

RECEPTORS	GRID SIZES (*X*, *Y*, *Z*)	GRID CENTERS		
		X	*Y*	*Z*
Dengue NS2B/NS3	40 × 40 × 40	0.456	−17.036	13.989
Dengue NS5	40 × 40 × 40	24.892	162.151	24.605
COVID RdRP	40 × 40 × 40	121.499	123.272	127.073
Influenza RdRP	40 × 40 × 40	98.433	−4.413	−9.268

Docking

AutoDock Tools 1.5.6 was used for the docking, which has a rapid processing time and accurately anticipates binding places, and determines the grid box dimensions automatically.[51] In the present study, the grid spacing of 0.375 Å was used for all receptor proteins. The grid center and grid box size are given in Table 1. A set of commands were entered into the command prompt to create the output scores and start the docking analysis. The data showed the binding affinity in kilocalories, and the ligand with the lowest value was assumed to have the greatest binding interactions.[52] The docking complexes were visualized in UCSF ChimeraX[53,54] and their binding interactions were examined in Discovery Studio.[55]

Molecular dynamic simulations

In this investigation, we conducted molecular dynamics (MD) simulations on a grapjics processing unit (GPU)-accelerated platform using the GROMACS software package.[56] The system was prepared utilizing the CHARMM-GUI solution builder,[57] and the resulting input files were exported in the Gromacs format. Initialization of particle positions was performed using the Gromacs.gro file, while the interactions between particles were defined using a topology file. Long-range electrostatic interactions were evaluated employing the particle mesh Ewald method, and a cutoff distance of 1.2 nm was implemented for van der Waals interactions. The equilibration of the system was carried out in the isothermal-isobaric ensemble, followed by the final simulation in the canonical ensemble, maintaining a temperature of 300 K for a duration of 50 ns. The simulation was executed using a Langevin integrator with a timestep of 1 fs. For trajectory analysis, we utilized the MD analysis package[58] to compute crucial parameters, including the root mean square fluctuation (RMSF), radius of gyration (Rg), and root mean square deviation (RMSD) of both the protein and protein-ligand complexes. These parameters facilitated the assessment of deviations and stability of the protein and complexes throughout the simulation.[58]

Results

Ligand retrieval

From *B lycium* bioactive constituents, ie, berberine (CID_2353), berbamine (CID_275182), berbamunine (CID_440585), oxyberberine (CID_11066), oxyacanthine (CID_442333), baluchistanamine (CID_102267542), sindamine (CID_102512444), punjabine (CID_101428301), and jhelumine (CID_102148948), were selected. The following investigation additionally incorporated two standard antiviral drugs, ie, remdesivir (CID_121304016) and favipiravir (CID_492405). The physicochemical properties of the selected phytocompounds and the reference drugs are given in Table 2.

Pharmacokinetic analysis

Prediction of ADME properties. When assessing the ability of a drug to spread throughout the body, the BBB must be taken into consideration. Berberine and oxyberberine were shown to be able to pass the BBB, according to the ADME study of understudied phytoconstituents (Table 3). However, all the other chosen phytoligands and reference antiviral drugs had negative findings, indicating that they are unable to cross BBB. The results also indicate that maximum phytoconstituents are P-gp substrates, except berbamine, berbamunine, oxyberberine, and antiviral drug favipiravir. The studied substances were predicted to suppress the five classes of cytochromes P450 for continuous plasma concentrations and improved bioavailability. Berberine and oxyberberine were capable of suppressing CYP1A2, CYP2D6, and CYP3A4. CYP2C9 was inhibited by baluchistanamine, sindamine, punjabine, and oxyberberine. Among the antiviral drugs, remdesivir had shown to inhibit CYP3A4 only. Except for the antiviral medication remdesivir which has shown low human intestinal absorption, all remaining phytonutrients and favipiravir showed high GI absorption suggesting more than 95% chance of being absorbed by the human intestine.

Drug-likeness analysis. The most crucial factor in evaluating the bioavailability of the understudy phytochemicals is drug-likeness prediction. Lipinski rule, Ghose rule, Veber rule, Egan rule, and Muegge rule are summed up in Table 4. Only two phytocompounds, ie, berberine and oxyberberine, showed zero Lipinski violation and followed all the parameters set in Ghose, Veber, Egan, and Muegge filter. Berbamine, berbamunine, baluchistanamine, and sindamine have MWs higher than the permissible range (<500 Da) indicating passing the Lipinski rule with one Lipinski violation along with three Ghose violations. While following the Egan rule and Veber rule, berbamine, sindamine, and baluchistanamine showed two Muegge violations whereas berbamunine had one violation. Among antiviral drugs, favipiravir showed no Lipinski violation but four Ghose and one Muegge violations. Remdesivir has surprisingly depicted two Lipinski, three Ghose, two Veber, one Egan, and three Muegge violations by exceeding the permissible limit of hydrogen-bond acceptor and topological surface area.

The understudy compounds have been subjected for bioactivity score evaluation and their results are summarized in Table 5. Berberine showed promising bioactivity as ion channel modulator and enzyme inhibitor and was moderately active as

Table 2. Physicochemical properties of the selected phytocompounds and the reference drugs.

LIGANDS	CLASS OF COMPOUND	PUBCHEM CID	MOLECULAR FORMULA	STRUCTURES	CONICAL SMILES
Berberine	Alkaloids	CID_2353	$C_{20}H_{18}NO_4^+$	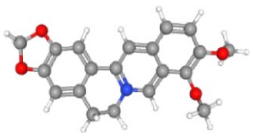	COC1=C(C2=C[N+]3=C(C=C2C=C1)C4=CC5=C(C=C4CC3)OCO5)OC
Berbamine	Alkaloids	CID_275182	$C_{37}H_{40}N_2O_6$	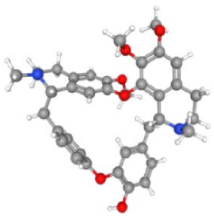	CN1CCC2=CC(=C3C=C2[C@@H]1CC4=CC=C(C=C4)OC5=C(C=CC(=C5)C[C@@H]6C7=C(O3)C(=C(C=C7CCN6C)OC)OC)O)OC
Berbamunine	Alkaloids	CID_440585	$C_{36}H_{40}N_2O_6$	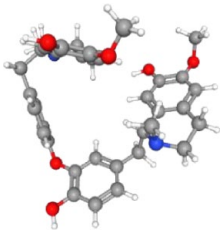	CN1CCC2=CC(=C(C=C2[C@@H]1CC3=CC=C(C=C3)OC4=C(C=CC(=C4)C[C@@H]5C6=CC(=C(C=C6CCN5C)OC)O)O)O)OC
Oxyberberine	Alkaloids	CID_11066	$C_{20}H_{17}NO_5$	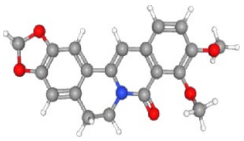	COC1=C(C2=C(C=C1)C=C3C4=CC5=C(C=C4CCN3C2=O)OCO5)OC
Oxyacanthine	Phenols	CID_442333	$C_{37}H_{40}N_2O_6$	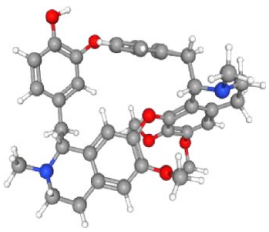	CN1CCC2=CC(=C(C3=C2[C@@H]1CC4=CC=C(C=C4)OC5=C(C=CC(=C5)C[C@@H]6C7=CC(=C(C=C7CCN6C)OC)O3)O)OC)OC
Baluchistanamine	Alkaloids	CID_102267542	$C_{37}H_{38}N_2O_8$	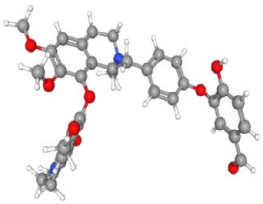	CN1CCC2=CC(=C(C(=C2[C@@H]1CC3=CC=C(C=C3)OC4=C(C=CC(=C4)C=O)O)OC5=C(C=C6CCN(C(=O)C6=C5)C)OC)OC)OC
Sindamine	Alkaloids	CID_102512444	$C_{37}H_{38}N_2O_8$	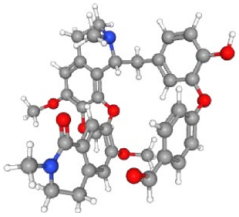	CN1CCC2=CC(=C(C(=C2[C@H]1CC3=CC(=C(C=C3)O)OC4=CC=C(C=C4)C=O)OC5=C(C=C6CCN(C(=O)C6=C5)C)OC)OC)OC

(Continued)

Table 2. (Continued)

LIGANDS	CLASS OF COMPOUND	PUBCHEM CID	MOLECULAR FORMULA	STRUCTURES	CONICAL SMILES
Punjabine	Alkaloids	CID_101428301	$C_{35}H_{32}N_2O_7$	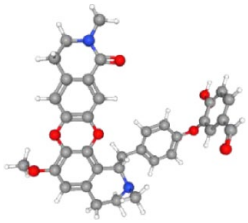	CN1CCC2=CC(=C3C(=C2[C@@H]1CC 4=CC=C(C=C4)OC5=C(C=CC(=C5) C=O)O)OC6=C(O3)C= (C(=O)C7=C6)C) OC
Jhelumine	Alkaloids	CID_102148948	$C_{36}H_{38}N_2O_7$	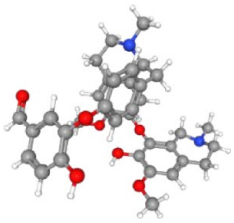	CN1CCC2=CC(=C(C(=C2C1) OC3=C(C=C4CCN([C@H](C4=C3) CC5=CC=C(C=C5)OC6=C(C=CC(=C6) C=O)O)C)OC)O)OC
Remdesivir	FDA-approved antiviral drug	CID_121304016	$C_{27}H_{35}N_6O_8P$	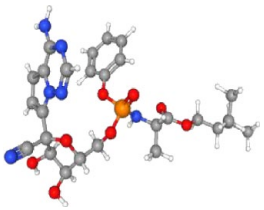	CCC(CC)COC(=O)[C@H](C)N[P@](=O) (OC[C@@H]1[C@H]([C@H]([C@](O1) (C#N)C2=CC=C3N2N=CN=C3N)O)O) OC4=CC=CC=C4
Favipiravir	FDA-approved antiviral drug	CID_492405	$C_5H_4FN_3O_2$	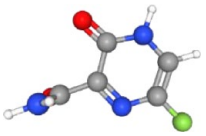	C1=C(N=C(C(=O)N1)C(=O)N)F

Abbreviations: CID, compound identification; FDA, food and drug administration

GPCR ligand, kinase, and protease inhibitor. Oxyberberine was moderately active as ion channel modulator, nuclear receptor ligand, and protease inhibitor while the bioactivity score above 0.0 indicated high activity as GPCR ligand, kinase inhibitor, and enzyme inhibitor. Baluchistanamine and sindamine have shown identical scores, both were moderately active as GPCR ligand and protease inhibitor but inactive as ion channel modulator, kinase inhibitor, nuclear receptor inhibitor, and enzyme inhibitor. Remdesivir was active as GPCR ligand, kinase inhibitor, protease inhibitor, and enzyme inhibitor and moderately active as ion channel modulator and nuclear receptor ligand. Favipiravir was moderately active as ion channel modulator, kinase inhibitor, and enzyme inhibitor but remained inactive as GPCR ligand, nuclear receptor ligand, and protease inhibitor.

Toxicity analysis. The toxicity risk assessment (Table 6) revealed that berberine, berbamine, berbamunine, oxyacanthine, and sindamine were found to be non-toxic in terms of mutagenicity, tumorigenicity, reproductive toxicity, and irritant. Oxyberberine possesses reproductive toxicity factor whereas punjabine was slightly mutagenic and irritant. Baluchistanamine and jhelumine also occurred to be irritants. Favipiravir was non-mutagenic, non-tumorigenic, and safe for reproductive system but a positive irritant. Remdesivir, on the other hand, was non-mutagenic but highly positive as tumorigenic, reproductive toxin, and irritant. Berbamine, berbamunine, oxyberberine, oxyacanthine, baluchistanamine, sindamine, punjabine, and jhelumine showed drug-likeness score greater than 1, while berberine presented negative value for drug-likeness. For remdesivir drug-likeness, value was recorded to be 2.9436 while the highest negative value was recorded for favipiravir, ie, –21.38.

Docking analysis

Docking between the receptor proteins and selected phytoligands by AutoDock Vina returned energies in kcal/mol and highest negative value for each pair is shown in Table 7. For Dengue NS2BNS3, highest binding affinity was recorded with punjabine (ie, –10.9 kcal/mol) followed by jhelumine (–9.3 kcal/mol). Binding energy obtained for oxyacanthine and sindamine was –9.1 and –9.0 kcal/mol, respectively. Berberine and berbamine bound with same affinity (–8.0 kcal/mol). Among the antiviral drugs, remdesivir showed binding energy –7.7 kcal/mol and favipiravir showed –5.8 kcal/mol. The binding

Table 3. Pharmacokinetics of selected phytoligands of *B lycium* and standard antiviral drugs (ie, remdesivir and favipiravir).

LIGANDS	GI ABSORPTION	BBB PERMEANT	P-GP SUBSTRATE	CYP1A2 INHIBITOR	CYP2C19 INHIBITOR	CYP2C9 INHIBITOR	CYP2D6 INHIBITOR	CYP3A4 INHIBITOR
Berberine	High	Yes	Yes	Yes	No	No	Yes	Yes
Berbamine	High	No	No	No	No	No	No	No
Berbamunine	High	No	No	No	No	No	No	No
Oxyberberine	High	Yes	Yes	Yes	No	Yes	Yes	Yes
Oxyacanthine	High	No	No	No	No	No	No	No
Baluchistanamine	High	No	Yes	No	Yes	Yes	No	No
Sindamine	High	No	Yes	No	Yes	Yes	No	No
Punjabine	High	No	Yes	No	No	Yes	Yes	No
Jhelumine	High	No	Yes	No	No	No	No	No
Remdesivir	Low	No	Yes	No	No	No	No	Yes
Favipiravir	High	No	No	No	No	No	No	No

Abbreviations: BBB, blood-brain barrier; GI, gastrointestinal; P-gp, permeability glycoprotein.

Table 4. The drug-likeness properties (Lipinski rule) of the selected phytoligands and standard antiviral drugs (ie, remdesivir and favipiravir).

LIGANDS	MILOGP (≤5)	MW (≤500)	NOHNH (≤5)	NON (≤10)	TPSA (≤140 Å²)	LIPINSKI VIOLATIONS	GHOSE	VEBER	EGAN	MUEGGE
Berberine	0.20	336.37	0	5	40.82	0	Yes	Yes	Yes	Yes
Berbamine	3.55	608.74	1	8	72.87	1	No, 3 violations	Yes	Yes	No, 2 violations
Berbamunine	3.11	596.72	3	8	94.86	1	No, 3 violations	Yes	Yes	No, 1 violations
Oxyberberine	3.13	351.36	0	6	58.94	0	Yes	Yes	Yes	Yes
Oxyacanthine	6.24	608.74	1	8	72.87	2	No, 3 violations	Yes	Yes	No, 2 violations
Baluchistanamine	4.97	638.72	1	10	107.02	1	No, 3 violations	Yes	Yes	No, 2 violations
Sindamine	4.97	638.72	1	10	107.02	1	No, 3 violations	Yes	Yes	No, 2 violations
Punjabine	5.13	592.65	1	9	105.59	2	No, 3 violations	Yes	Yes	No, 1 violation
Jhelumine	5.53	610.71	2	9	100.94	2	No, 3 violations	Yes	Yes	No, 2 violations
Remdesivir	2.82	602.59	5	14	203.57	2	No, 3 violations	No, 2 violations	No, 1 violation	No, 3 violations
Favipiravir	−0.98	157.10	3	5	88.85	0	No, 4 violations	Yes	Yes	No, 1 violation

Abbreviations: MW, molecular weight; nOHNH, number of hydrogen bond donors; nON, number of hydrogen bond acceptors; TPSA, total polar surface area.

affinities of the understudy compounds and antiviral drugs with NS2BNS3 can be summarized in following ascending order: favipiravir < remdesivir < berberine = berbamine < oxyberberine < baluchistanamine < berbamunine < sindamine < oxyacanthine < jhelumine < punjabine.

For DENV NS5, the highest binding affinity was recorded for punjabine with energy −10.4 kcal/mol and berbamunine came next in line with energy −9.6 kcal/mol. Oxyberberine (−9.4 kcal/mol), berberine (−8.3 kcal/mol), and berbamine (−8.2 kcal/mol) have also shown very promising results. The

Table 5. Bioactivity scores of selected phytoligands and standard antiviral drugs.

LIGANDS	GPCR LIGAND	ION CHANNEL MODULATOR	KINASE INHIBITOR	NUCLEAR RECEPTOR LIGAND	PROTEASE INHIBITOR	ENZYME INHIBITOR
Berberine	−0.11	0.71	−0.27	−0.78	−0.35	0.82
Berbamine	−0.01	−0.61	−0.49	−0.56	−0.08	−0.32
Berbamunine	0.04	−0.51	−0.34	−0.37	0.00	−0.25
Oxyberberine	0.13	−0.16	0.07	−0.28	−0.10	0.03
Oxyacanthine	−0.01	−0.61	−0.49	−0.56	−0.08	−0.32
Baluchistanamine	−0.22	−0.95	−0.73	−0.80	−0.26	−0.56
Sindamine	−0.22	−0.95	−0.73	−0.80	−0.26	−0.56
Punjabine	−0.01	−0.63	−0.44	−0.38	−0.07	−0.20
Jhelumine	−0.05	−0.62	−0.51	−0.55	−0.15	−0.32
Remdesivir	0.27	−0.35	0.20	−0.48	0.49	0.38
Favipiravir	−0.62	−0.44	−0.31	−1.50	−0.91	−0.33

Abbreviation: GPCR, G protein-coupled receptor.

Table 6. Toxicity risk analysis of selected phytochemicals and standard antiviral drugs.

LIGANDS	DRUG-LIKENESS	MUTAGENIC	TUMORIGENIC	EFFECTS ON REPRODUCTIVE SYSTEM	IRRITANT	CARCINOGENIC
Berberine	−2.2467					
Berbamine	4.6261					
Berbamunine	4.6261					
Oxyberberine	3.5103					
Oxyacanthine	4.6261					
Baluchistanamine	3.2233					
Sindamine	3.2233					
Punjabine	3.2233					
Jhelumine	3.2061					
Remdesivir	2.9436					
Favipiravir	−21.381					

Note. Red: highly toxic; yellow: slightly toxic; green: Non toxic.

lowest binding affinity was exhibited by the antiviral drug favipiravir with energy −6.2 kcal/mol. The binding affinities of the understudy compounds and antiviral drugs with NS5 can be summarized in following ascending order: favipiravir < sindamine < jhelumine < berbamine ⩽ oxyacanthine = baluchistanamine < berberine < remdesivir < oxyberberine < berbamunine < punjabine.

The docking analysis of COVID RdRP with selected phytoligands revealed the highest binding affinity of oxyacanthine and baluchistanamine having the binding energy −9.5 kcal/mol. Punjabine exhibited the binding energy of −9.1 kcal/mol, whereas berbamine and sindamine displayed same binding energy, ie, −8.3 kcal/mol. All selected phytocompounds from *B lycium* showed stronger binding affinities than the chosen antiviral drugs. The binding energies obtained from berberine (−7.7 kcal/mol), berbamunine (−7.6 kcal/mol), oxyberberine (−7.8 kcal/mol), and jhelumine (−7.4 kcal/mol) were lower than remdesivir (−7.3 kcal/mol) and favipiravir (−5.2 kcal/mol) exhibiting higher binding affinity with COVID RdRP. The ascending order of binding affinities of the understudy

Table 7. Docking between the receptor proteins and selected phytoligands by AutoDock Vina.

LIGANDS	RECEPTORS			
	DENGUE NS2B/NS3	DENGUE NS5	COVID RDRP	INFLUENZA RDRP
Berberine	−8.0	−8.3	−7.7	−8.3
Berbamine	−8.0	−8.2	−8.3	−9.2
Berbamunine	−8.9	−9.6	−7.6	−10.2
Oxyberberine	−8.2	−9.4	−7.8	−8.6
Oxyacanthine	−9.1	−8.2	−9.5	−9.4
Baluchistanamine	−8.6	−8.2	−9.5	−8.9
Sindamine	−9.0	−7.5	−8.3	−8.8
Punjabine	−10.9	−10.3	−9.1	−10.4
Jhelumine	−9.3	−8.0	−7.4	−9.1
Remdesivir	−7.7	−8.5	−7.3	−8.5

phytocompounds and antiviral drugs with COVID RdRP can be summarized as following: favipiravir < remdesivir < jhelumine < berbamunine < berberine < oxyberberine < berbamine = sindamine < punjabine < oxyacanthine = baluchistanamine.

Docking between the influenza RdRP and the selected phytochemicals of *B lycium* returned promising results as all the compounds showed stronger binding affinity than antiviral drug favipiravir (−5.5 kcal/mol). Berberine (−8.3 kcal/mol) has shown binding energies higher than remdesivir (−8.5 kcal/mol) reflecting the higher affinity of the drug. Berbamine (−9.2 kcal/mol), oxyacanthine (−9.4 kcal/mol), berbamunine (−10.2 kcal/mol), and punjabine (−10.4 kcal/mol) have shown the best results with influenza RdRP. The ascending order of binding affinities of the understudy phytocompounds and antiviral drugs with influenza RdRP can be summed up as: favipiravir < berberine < remdesivir < oxyberberine < sindamine < baluchistanamine < jhelumine < berbamine < oxyacanthine < berbamunine < punjabine. The 3D structures of top three docking complexes of each viral proteins and phytoligands and their respective 2D lines models are given in Figures 2 to 5 and remaining structures are given in Supplemental Figure S1.

Molecular dynamic simulations

Considering the pharmacokinetic analyses, drug-likeness, Lipinski rule of five followed by bioavailability score, non-toxicity, and promising docking results, berberine ligand in complex with viral proteins (Figure 6) was chosen to perform MD simulations.

Figure 7 illustrates the RMSD graphs of the berberine ligand in complex with (A) DENV NS2B/NS3 protease, (B) DENV NS5 polymerase, (C) COVID-19 RdRP, and (D) influenza RdRP protein complex. The RMSD curves were collected based on the MD trajectory after the experiment. The RMSD of the DENV NS2B/NS3 protease complex showed minor fluctuations between 0 and 1000 ps, which is an acceptable range, and remained stable at 1.0 to 1.2 nm up to 20 000 ps (2 ns), followed by minor fluctuations before 5 ns. The influenza RdRP protein complex had the highest fluctuation wavelength of 3.0 nm, while the DENV NS2B/NS3 protease complex had the lowest fluctuation wavelength up to 1.4 nm. All complexes showed an increase in fluctuation reaching a peak value between 4 and 5 ns of the simulation. Figure 7 shows that all complexes had very stable binding site structures. RMSD is a commonly used measure of the differences between the structures sampled during simulation and the reference structure.

Based on the above speculation, the variation of Rg during MD simulation was probably caused by the binding site of the target and ligand (Figure 8). The Rg indicates protein stability during simulation. In other words, the Rg curve of a well-folded protein reaches a plateau during simulation. Rg fluctuation can be used to monitor changes in protein structure. Figure 2 shows the Rg graphs of the berberine ligand in complex with (A) DENV NS2B/NS3 protease, (B) DENV NS5 polymerase, (C) COVID-19 RdRP, and (D) influenza RdRP protein complex. The average Rg values show that the influenza RdRP protein had the highest Rg, followed by COVID-19 RdRP, DENV NS5 polymerase, and DENV NS2B/NS3 protease with the lowest Rg value. The plot of COVID-19 RdRP was similar to that of the DENV NS5 polymerase complex, with fluctuations between 2 and 3 ns. Figure 8 reveals that all complexes had very stable binding site structures.

Figure 9 shows the RMSF graphs of the berberine ligand in complex with (A) DENV NS2B/NS3 protease, (B) DENV NS5 polymerase, (C) COVID-19 RdRP, and (D) influenza

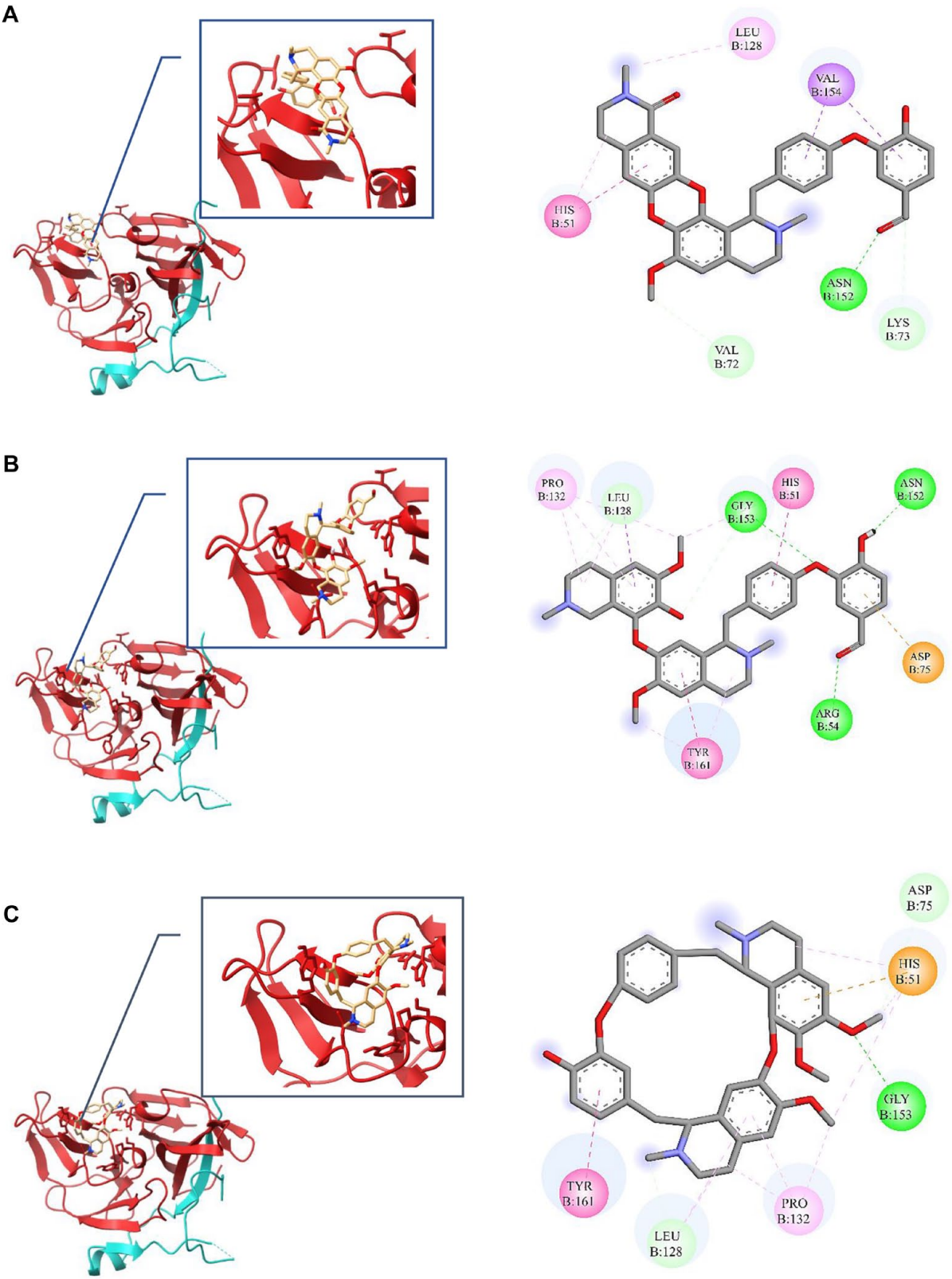

Figure 2. The 3D structures (left) and their 2D line models (right) of top three docking complexes of NS2BNS3 and selected phytocompounds from *B lycium*. (A) NS2BNS3-punjabine, (B) NS2BNS3-jhelumine, and (C) NS2BNS3-oxyacanthine.

RdRP protein complex. The RMSF plot of the DENV NS2B/NS3 protease-berberine complex showed little fluctuation compared to other complexes, with no abrupt differences in the plot. The high flexibility values were found at residues 38 and 110 of the DENV NS2B/NS3 protease-berberine complex, between residues 200 and 400 for the COVID-19

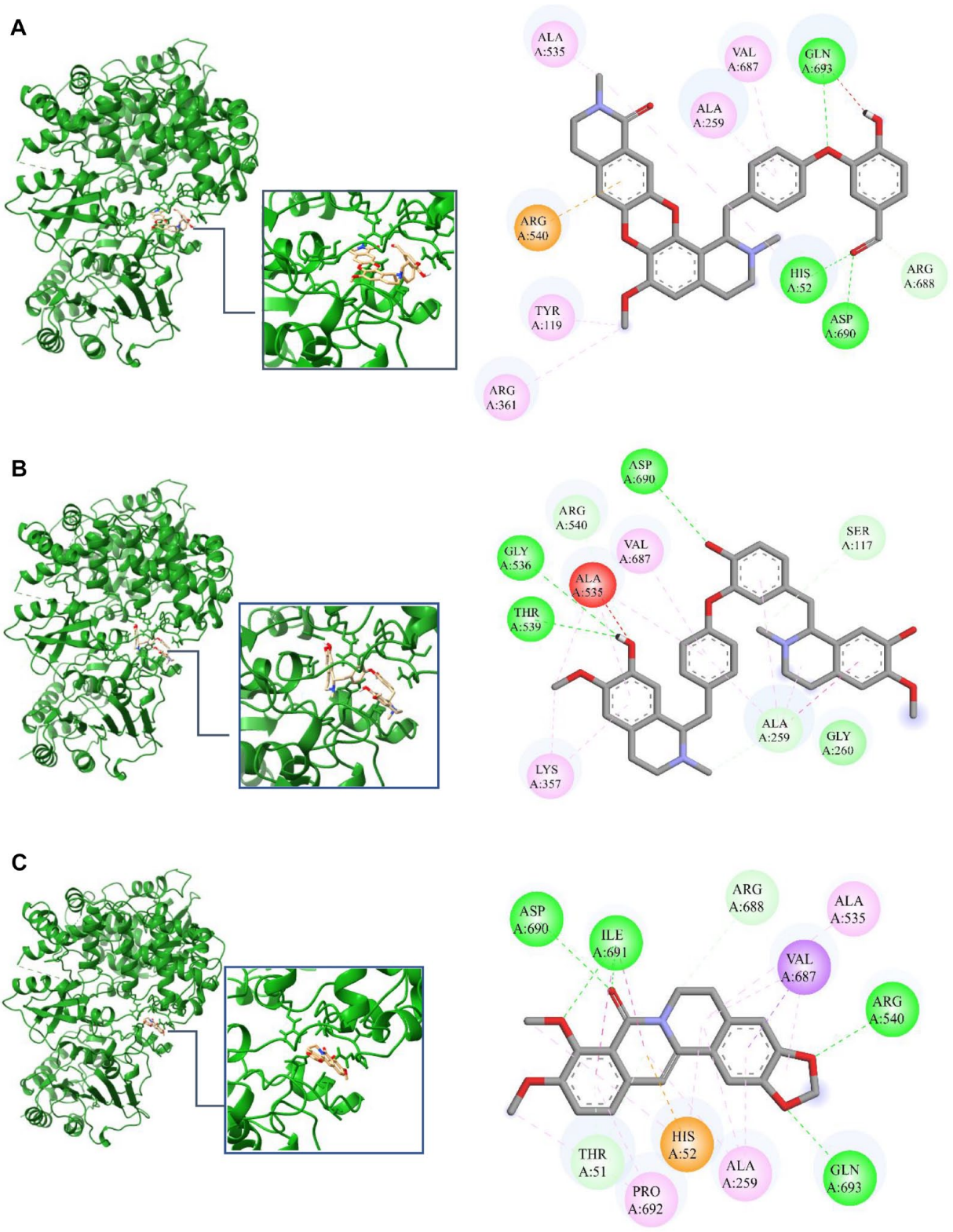

Figure 3. The 3D structures (left) and their 2D line models (right) of top three docking complexes of NS5 and selected phytocompounds from *B lycium*. (A) NS2BNS3-punjabine, (B) NS2BNS3-berbamumine, and (C) NS2BNS3-oxyberberine.

RdRP-berberine complex, residue 500 for the DENV NS5 polymerase-berberine complex, and residue 430 for the influenza RdRP protein-berberine complex. RMSF measures the movement of a subset of atoms with respect to the average structure over the entire simulation and indicates the flexibility of different regions of a protein. RMSF can be used to evaluate structural movement and flexibility. The binding site is mainly composed of several key residues in the active pocket, and

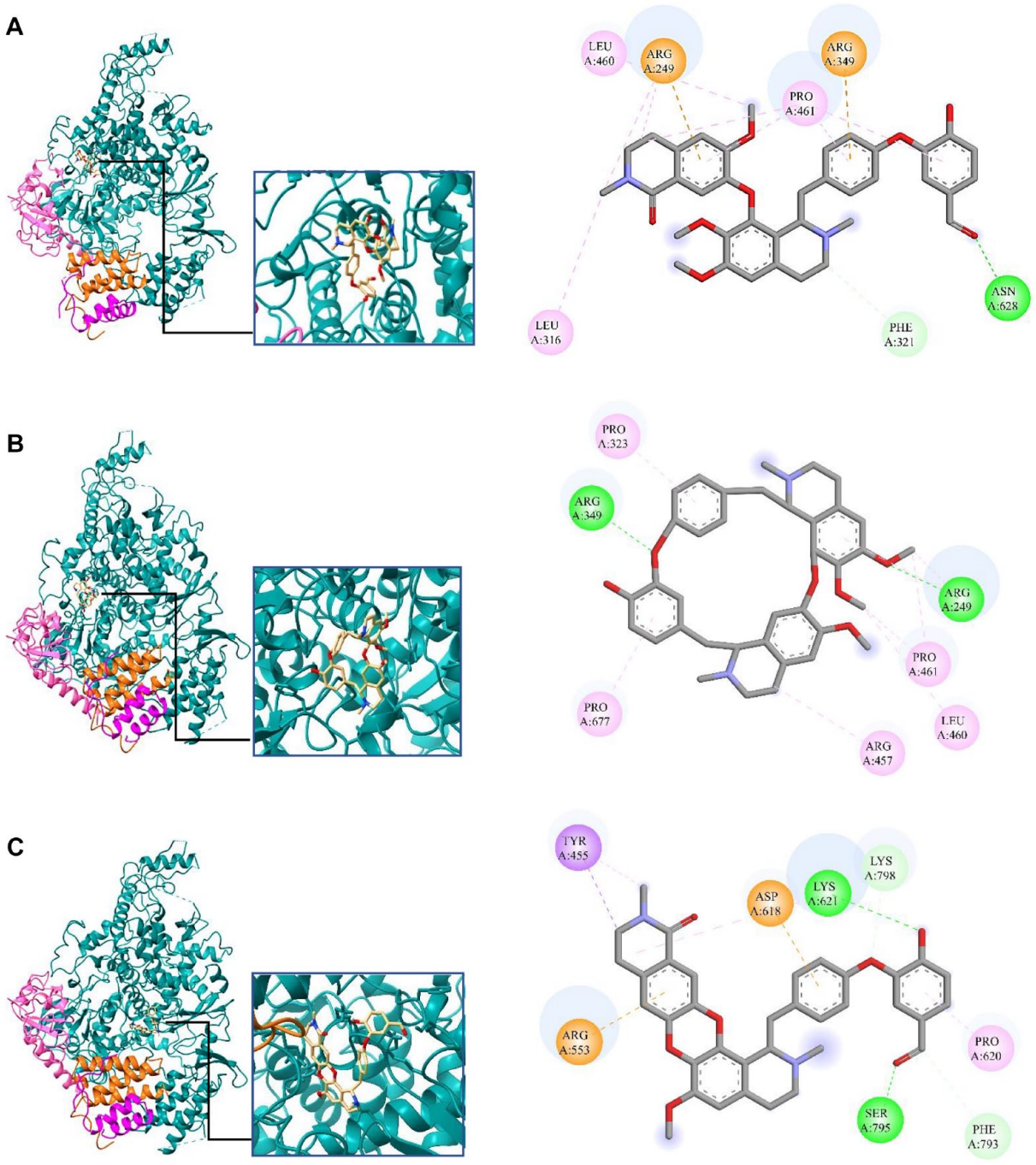

Figure 4. The 3D structures (left) and their 2D line models (right) of top three docking complexes of COVID RdRP and selected phytocompounds from *B lycium*. (A) NS2BNS3-baluchistanamine, (B) NS2BNS3-oxyacanthine, and (C) NS2BNS3-punjabine.
Abbreviation: RdRP, RNA-dependent RNA polymerase.

monitoring the behavior of these residues can contribute to the study of protein-ligand interactions.

Discussion

The influenza virus and the SARS-CoV-2 are two respiratory viruses that have sporadically caused global pandemics. While the influenza virus has been kept under control for a while, seasonal influenza still claims numerous lives every year, and sometimes a pandemic influenza virus appears.[59] Several breakouts of different serotypes of the DENV and its global expansion have led to a significant number of fatalities as well as a medical emergency because no effective treatments for DENV infections have yet been discovered. The COVID-19 issue and dengue illness outbreaks in several regions are difficulties that the entire globe is now battling. The majority of epidemic and pandemic viral illnesses have caused enormous destruction and

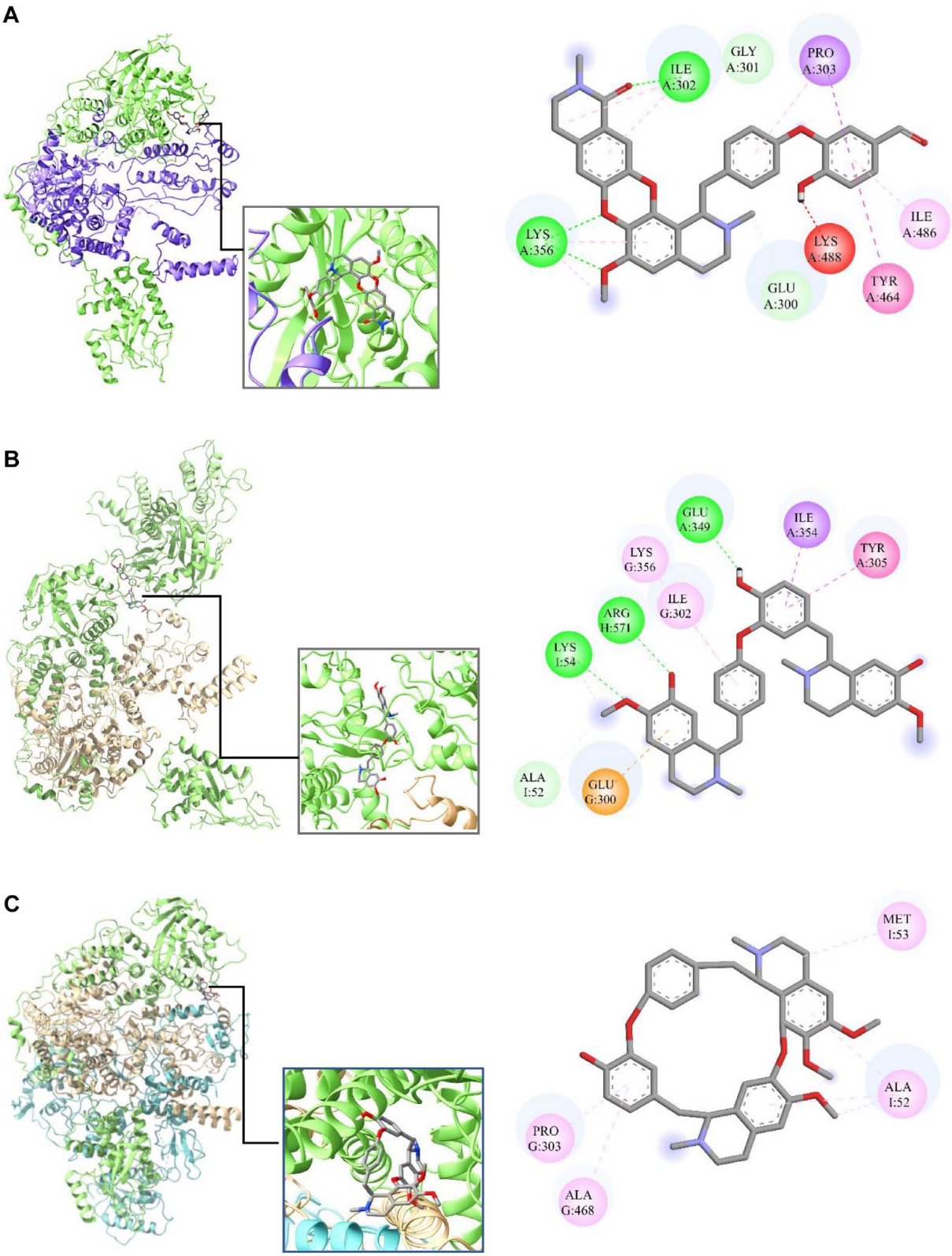

Figure 5. The 3D structures (left) and their 2D line models (right) of top three docking complexes of influenza RdRP and selected phytocompounds from *B lycium*. (A) NS2BNS3-punjabine, (B) NS2BNS3-berbamumine, and (C) NS2BNS3-oxyacanthine.
Abbreviation: RdRP, RNA-dependent RNA polymerase.

countless lives during the past several decades.[60] The populace as well as the country's healthcare system are suffering greatly as a result of the simultaneous load of dengue and COVID-19.[9,61] Considering that RNA viruses have high mutation rates, developing vaccines against them is extremely difficult or almost impossible. Novel antiviral medicines generated from plants may be considered as effective alternatives in the fight against this menace to humanity. These are believed to be

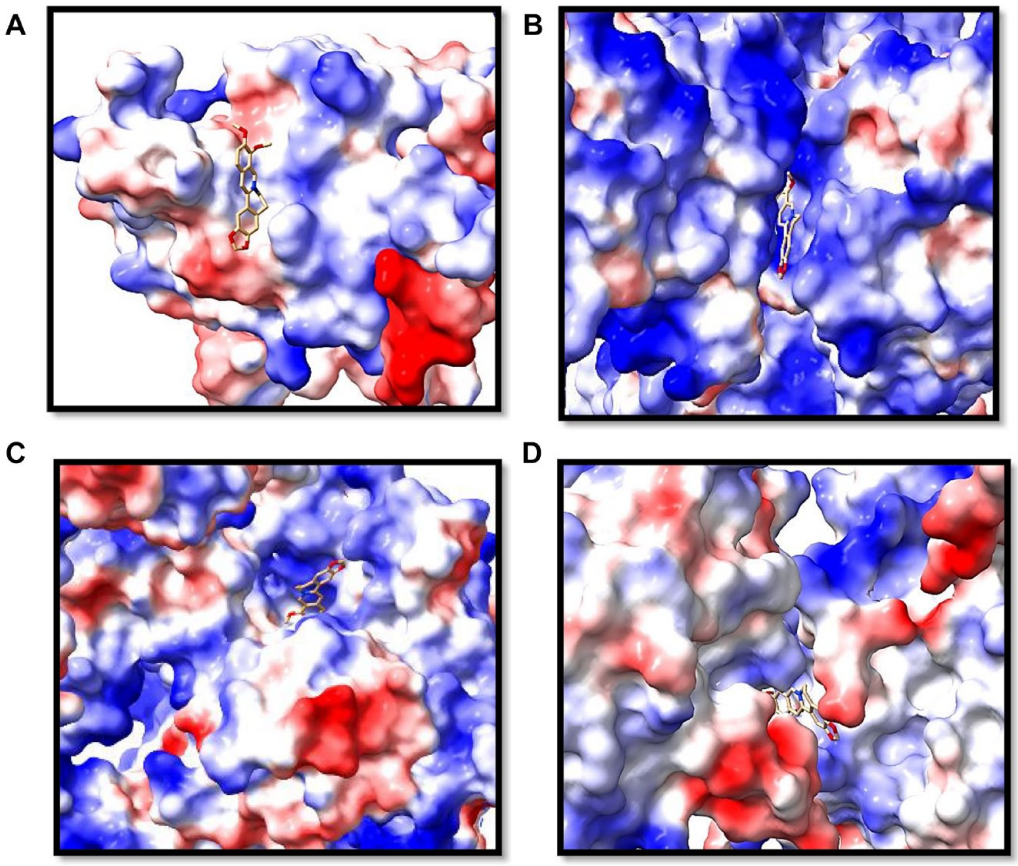

Figure 6. Illustration of the berberine ligand in complex with (A) DENV NS2B/NS3 protease, (B) DENV NS5 polymerase, (C) COVID-19 RdRP, and (D) influenza RdRP protein complex.
Abbreviation: RdRP, RNA-dependent RNA polymerase.

substances which have been utilized since the dawn of human civilization and are nontoxic, less threatening, and safe.

Historically, medicinal plants have been utilized to treat a range of human illnesses. The majority of Asian countries, including China, Japan, and India, have a long history of using extracts from medicinal plants and mushrooms. Medicinal plants have a significant number of therapeutically useful secondary metabolites that are of pharmacological importance. Many plant components or extracts have been used by locals to avoid several ailments since the very beginning and are still used now.[62,63] *B lycium* Royle, a member of the Berberidaceae family, a potent medicinal plant with a known history of use in ethnomedicine, has produced notable therapeutic effects in indigenous communities all over the world. In several regions of Pakistan, it is still used to cure chest issues, coughs, GI cramps, and diarrhea. Many biologically active substances, including alkaloids, saponins, tannins, berberine, berbamine, and sindamine, are found in *B lycium* and may be obtained from the plant's various parts.[25,64] The plant includes the isoquinoline alkaloid berberine and the main alkaloid umbellitine. This is often extracted from the roots or root bark of *B lycium* and other Berberis species that are widely distributed in nearby woodlands. This chemical has a wide range of biological uses, including antioxidant, anti-microbial, anti-inflammatory, anticancer, anti-diabetic, anti-hyperlipidemic, and hepatoprotective. For many years, the traditional medical system employed the roots of *B lycium* Royle to cure a variety of viral illnesses (ie, COVID-19, HCV, influenza, H1N1, enterovirus 71), bone and skin conditions, jaundice, ulcers, gonorrhea, diabetes, and blood pressure.[32,65,66] The current study investigated the antiviral potentials of 11 bioactive compounds, ie, berberine, berbamine, berbamunine, oxyberberine, oxyacanthine, baluchistanamine, punjabine, jhelumine and sindamine through pharmacokinetic and molecular dynamic studies.

Physicochemical and biopharmaceutical qualities that are acceptable for pharmaceutical development of a chemical entity should be combined with its potential pharmacological action in order to achieve the necessary pharmacokinetic parameters.[67] The process of absorption is where the supplied phytochemicals are first transferred. All understudied compounds were discovered to have a higher GI tract absorption, indicating a higher degree of water solubility. As a medication is absorbed, it must go through a distribution process that entails the permeability of the molecule and characterizes the compound's whole bioactivity. In general, only a tiny portion of the molecules provided for dispersion really reach the target in

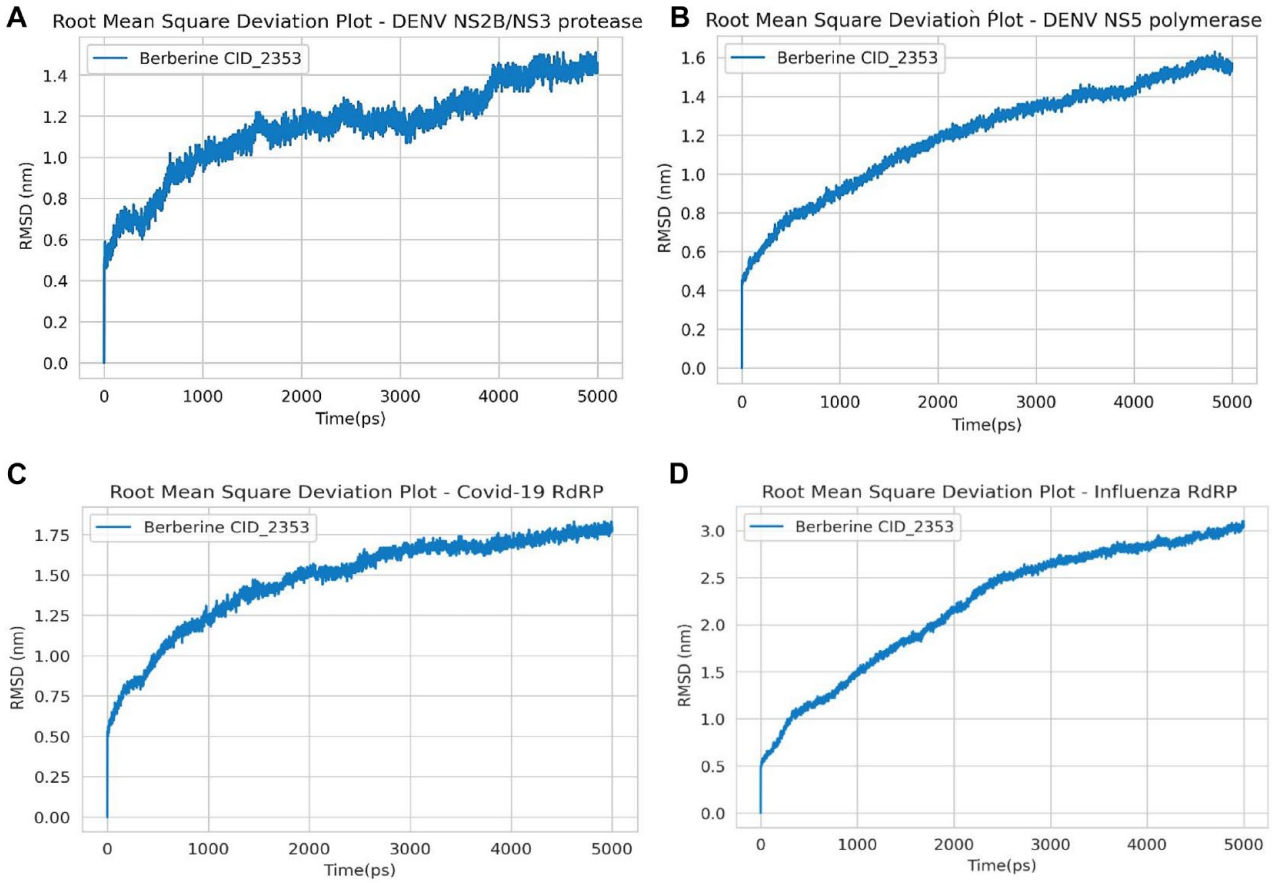

Figure 7. RMSD graph of ligand berberine and (A) DENV NS2B/NS3 protease, (B) DENV NS5 polymerase, (C) COVID-19 RdRP, and (D) influenza RdRP protein complex.
Abbreviations: RdRP, RNA-dependent RNA polymerase; RMSD, root mean square deviation.

full; the majority disintegrate before they do. The compound's bioactivity therefore seems to be diminished.[68] Knowledge about whether substances are substrate or non-substrate for the P-gp informs us about its active efflux across biological membranes, such as the GI wall to the lumen or from the brain. It is vital to know how compounds interact with cytochromes P450 since this enzyme is crucial for the metabolic biotransformation that leads to medication clearance. Thus, it is crucial for drug discovery to foresee a molecule's propensity to inhibit CYPs.[69,70] Swiss-ADME prediction in Table 3 revealed that all understudy phytoconstituents except berbamine, berbamunine, and oxyberberine were P-gp substrates and only berberine and oxyberberine were found capable of crossing BBB and suppressing cytochromes (CYP1A2, CYP2D6 and CYP3A4). The Lipinski rule of five, Ghose, Veber, Egan, and Muegge and bioavailability score were used to evaluate the drug-likeness. Only oral drugs are permitted to be evaluated when the lead molecules fulfill Lipinski criterion of five with no violations or a maximum of one violation.[71,72] Berberine and oxyberberine met the requirements of Ghose, Veber, Egan, and Muegge rules while not showing any signs of Lipinski violation suggests their potential as ideal lead compounds. Berberine and oxyberberine passed all the filters of pharmacokinetics analysis by exhibiting drug-likeness, excellent bioavailability, and non-toxic profile.

All the understudy compounds have shown strong binding affinity with the receptor DENV NS2BNS3, NS5, COVID RdRP, and influenza RdRP proteins. The top phytochemicals identified by the binding energy values in the AutoDock 1.5.6 program were taken into consideration based on their binding location and probable interactions with the major residues.[73,74] The conformations with the lowest connection affinities (less than –7.0 kcal/mol) were chosen as best after the docking procedure to further monitor interacting residues (Figures 2-4). Punjabine has shown the strongest binding affinity with NS2BNS3 (–10.9 kcal/mol), NS5 (–10.3 kcal/mol), and influenza RdRP (–10.4 kcal/mol). For COVID RdRP, the strongest binding affinity was possessed by oxyacanthine and baluchistanamine by having the lowest binding energy (–9.5 kcal/mol). The optimal pharmacokinetics, bioavailability, and safety profile of berberine also included lowered binding energy with –8.0 kcal/mol, NS5 (–8.3 kcal/mol), COVID RdRP (–7.7 kcal/mol), and influenza RdRP (–8.3 kcal/mol). Also, these substances have been contrasted with the common medications

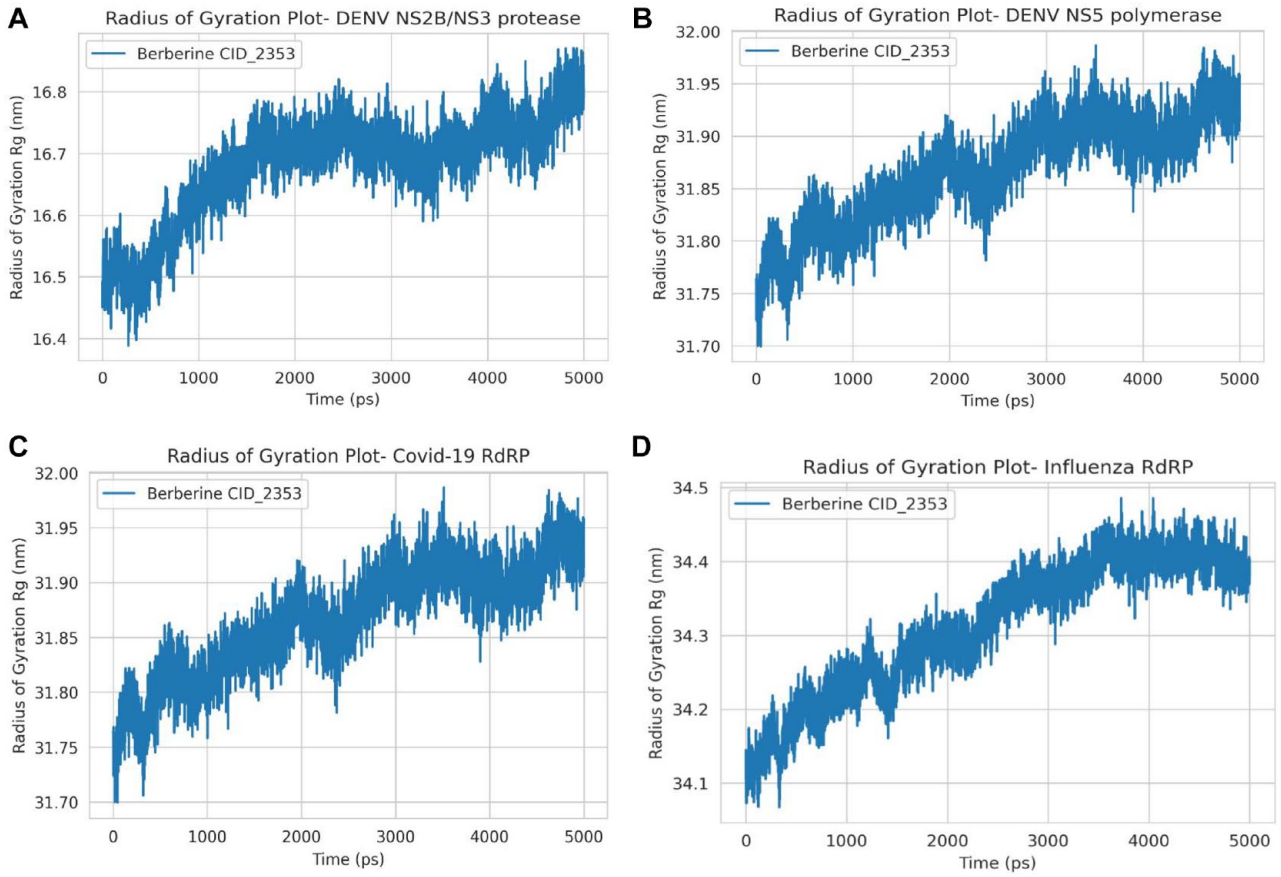

Figure 8. Radius of gyration graph of ligand berberine and (A) DENV NS2B/NS3 protease, (B) DENV NS5 polymerase, (C) COVID-19 RdRP, and (D) influenza RdRP protein complex.
Abbreviation: RdRP, RNA-dependent RNA polymerase.

remdesivir and favipiravir, indicating more hopeful outcomes for the research substances. The conformational changes of proteins and their interactions with ligands may be studied effectively using MD modeling. The RMSD plot is one of the methods most frequently employed to quantify the structural changes in proteins and to evaluate the stability of the protein-ligand complex during MD simulations. In this graph, the simulation duration is shown against the RMSD of the protein backbone, which is computed for each time step.[75,76]

The influenza RdRP protein complex exhibited the highest fluctuation wavelength of 3.0 nm, while the DENV NS2B/NS3 protease complex had the lowest fluctuation wavelength up to 1.4 nm. All complexes showed an increase in fluctuation reaching a peak value between 4 and 5 ns of the simulation. The structural variations among all the protein targets can account for this finding. Because of its flexibility, the protein target might adopt many conformations during the simulation, increasing the RMSD values.[77] The variation in RMSD values during the simulation can also be attributed to the specific binding interactions between the protein and ligand. Previous studies have shown that the RMSD of a ligand can be affected by the conformational changes of the protein side chains that form hydrogen bonds or van der Waals interactions with the ligand.[78,79] Therefore, differences in the binding interactions of different protein target with berberine may also contribute to the differences in their RMSD values. In summary, the RMSD plot of the MD simulation provides valuable information about the stability and conformational changes of the protein-ligand complex.

The RMSF is a commonly used measure in MD simulations to evaluate the flexibility of different regions of a protein. According to the simulation results, the RMSF values were calculated for berberine in complex with DENV NS2B/NS3 protease, DENV NS5 polymerase, COVID-19 RdRP, and influenza RdRP protein target. The high flexibility values were found at residues 38 and 110 of the DENV NS2B/NS3 protease-berberine complex, between residues 200 and 400 for the COVID-19 RdRP-berberine complex, residue 500 for the DENV NS5 polymerase-berberine complex, and residue 430 for the influenza RdRP protein-berberine complex. As noted by Gowers et al, understanding the flexibility of a protein structure is crucial for predicting protein-ligand interactions and for the

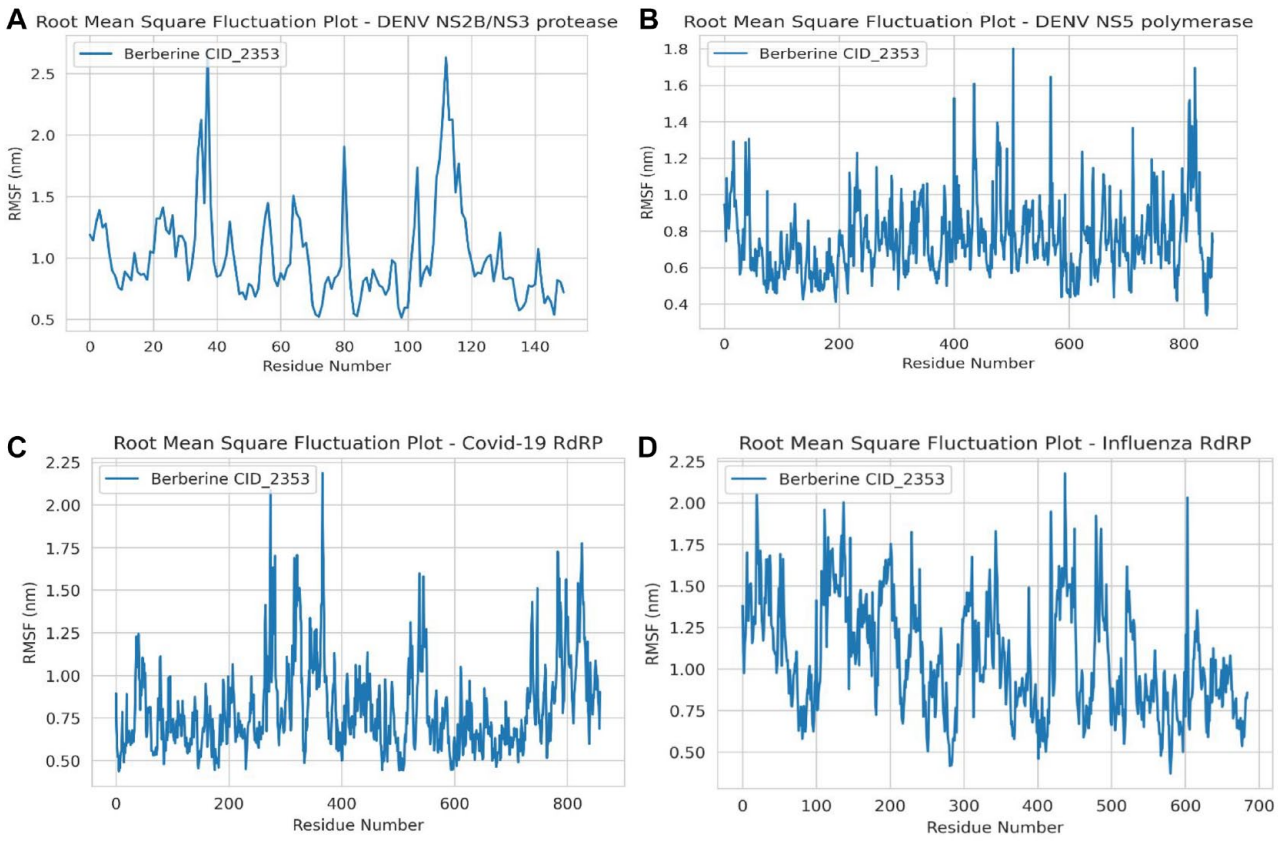

Figure 9. RMSF graph of ligand berberine and (A) DENV NS2B/NS3 protease, (B) DENV NS5 polymerase, (C) COVID-19 RdRP, and (D) influenza RdRP protein complex.
Abbreviations: RdRP, RNA-dependent RNA polymerase; RMSF, root mean square fluctuation.

rational design of drugs. In addition, several studies have demonstrated the importance of monitoring the behavior of key residues in the active site, which may affect protein function and drug binding.[80] According to the results obtained, the RMSF analysis provided insights into the flexibility of the protein-ligand complexes and the behavior of berberine in the presence of different four protein targets. Although the average RMSF values were similar between the complexes, the high flexibility values found in specific regions of the structure may have implications for protein-ligand interactions and drug binding. Overall, the RMSF plot provides valuable information about the flexibility of the protein structure during the simulation, which may impact protein-ligand interactions and drug design.

The Rg is a measure of the compactness of a protein and is commonly used to assess protein folding and stability during MD simulations. In our study, we analyzed the Rg values for the domains of our target proteins in complex with berberine using MD simulations.[81,82] The results indicate slight variations in the Rg values for different protein complexes. The DENV NS2B/NS3 protease exhibited the lowest Rg value, ranging from 16.4 to 16.9 nm. This suggests that the protease complex is relatively compact and tightly packed. The DENV NS5 polymerase and COVID-19 RdRP complexes showed similar Rg values, ranging from 31.7 to 32 nm. Both plot also show similar fluctuations between 2 and 3 ns, suggesting that berberine may have a slightly destabilizing effect on the protein structure and also shows that both complexes have a moderately extended conformation. In contrast, the influenza RdRP protein complex displayed the highest Rg value, ranging from 34.1 to 34.5 nm. This indicates a larger and more expanded conformation compared to the other complexes. The higher Rg value suggests that the influenza RdRP complex may have a more flexible structure with increased intermolecular distances. This observation is consistent with previous studies that have shown that ligand binding can affect protein stability and flexibility.[83] In addition, other factors such as temperature, solvent conditions, and simulation parameters can also influence Rg values and protein stability.[78] These results provide insights into the structural dynamics of the protein targets in a complex with berberine and highlight the potential impact of ligand binding on protein stability and flexibility.

Conclusion

A hidden treasure trove for antiviral research, berberine, berbamine, berbamunine, oxyberberine, oxyacanthine, baluchistanamine, and sindamine has showed encouraging findings

as possible lead compounds. *B lycium* phytocompounds can be used as lead compounds in the synthesis of novel antiviral medications. They are interesting candidates for further drug development procedures due to their proven effectiveness in blocking viral enzymes and advantageous pharmacokinetic characteristics. An encouraging approach to tackling the issue of drug resistance and the sluggish development of novel antiviral medications is the identification of potent phytocompounds. Compared to manufactured medications, natural substances frequently have distinct modes of action, which may assist address resistance problems. However, antiviral mechanisms of action of these phytochemicals are poorly known, and there are further investigations and clinical trials necessary for proving their effectiveness and toxicity in vivo. The therapeutic potential of naturally occurring substances derived from plants as antiviral medicines requires more investigation.

Acknowledgements

The authors acknowledge the support of the Department of Industrial Biotechnology at Atta-ur-Rahman School of Applied Biosciences, NUST, for providing the research facilities and funding.

Author Contributions

M.M. and H.A.K. conceptualized the study. Formal analyses were performed by M.M., T.A.I., and A.I.F. Validation was done by N.S.S.Z. and H.A.K. M.M. wrote the original draft. Original draft was reviewed and edited by N.S.S.Z. and H.A.K. All authors have read and agreed to the published version of the manuscript.

Ethical Approval

Ethical Approval is not applicable for this article.

Statement of Human and Animal Rights

This article does not contain any studies with human or animal subjects.

Statement of Informed Consent

There are no human subjects in this article and informed consent is not applicable.

ORCID iD


Mamuna Mukhtar https://orcid.org/0000-0002-5363-7342

SUPPLEMENTAL MATERIAL

Supplemental material for this article is available online.

REFERENCES

1. Adamson CS, Chibale K, Goss RJ, Jaspars M, Newman DJ, Dorrington RA. Antiviral drug discovery: preparing for the next pandemic. *Chem Soc Rev*. 2021;50:3647-3655.
2. Martinez JP, Sasse F, Brönstrup M, Diez J, Meyerhans A. Antiviral drug discovery: broad-spectrum drugs from nature. *Nat Prod Rep*. 2015;32:29-48.
3. Krishnan N, Devadasan V, Raman P. Plant-derived alkaloids as anti-viral agents. *Int J Res Pharm Sci*. 2020;11:6174-6182.
4. Abookleesh FL, Al-Anzi BS, Ullah A. Potential antiviral action of alkaloids. *Molecules*. 2022;27:903.
5. Mohan S, Elhassan Taha MM, Makeen HA, et al. Bioactive natural antivirals: an updated review of the available plants and isolated molecules. *Molecules*. 2020;25:4878.
6. Mei M, Tan X. Current strategies of antiviral drug discovery for COVID-19. *Front Mol Biosci*. 2021;8:671263. doi:10.3389/fmolb.2021.671263
7. Ngwe Tun MM, Toume K, Luvai E, et al. The discovery of herbal drugs and natural compounds as inhibitors of SARS-CoV-2 infection in vitro. *J Nat Med*. 2022;76:402-409.
8. Patel H, Kukol A. Integrating molecular modelling methods to advance influenza A virus drug discovery. *Drug Discov Today*. 2021;26:503-510.
9. Mukhtar M, Wajeeha AW, Bibi N. Engineering modified mRNA-based vaccine against dengue virus using computational and reverse vaccinology approaches. *Int J Mol Sci*. 2022;23:13911.
10. Delang L, Abdelnabi R, Neyts J. Favipiravir as a potential countermeasure against neglected and emerging RNA viruses. *Antiviral Res*. 2018;153:85-94.
11. Shiraki K, Daikoku T. Favipiravir, an anti-influenza drug against life-threatening RNA virus infections. *Pharmacol Ther*. 2020;209:107512.
12. Hickman MR, Saunders DL, Bigger CA, Kane CD, Iversen PL. The development of broad-spectrum antiviral medical countermeasures to treat viral hemorrhagic fevers caused by natural or weaponized virus infections. *PLoS Negl Trop Dis*. 2022;16:e0010220.
13. Dhama K, Karthik K, Khandia R, et al. Medicinal and therapeutic potential of herbs and plant metabolites/extracts countering viral pathogens-current knowledge and future prospects. *Curr Drug Metab*. 2018;19:236-263.
14. Bukhari SMF, Ali G. An overview of ethnobotany of *Berberis lycium* Royle in Pakistan. In: Öztürk M, Khan SM, Altay V, Efe R, Egamberdieva D, Khassanov FO, eds. *Biodiversity, Conservation and Sustainability in Asia*. Springer; 2022:931-942.
15. Ahmad M, Alamgeer ST. A potential adjunct to insulin: *Berberis lycium* Royle. *Diabetol Croat*. 2009;38:13-18.
16. Rahimi Madiseh M, Heidarian E, Rafieian-Kopaei M. Biochemical components of *Berberis lycium* fruit and its effects on lipid profile in diabetic rats. *J Herbmed Pharmacol*. 2014;3:15-19.
17. Shabbir A, Shahza DN, Arfat Y. *Berberis lycium* Royle: a review of its traditional uses, phytochemistry and pharmacology. *Afr J Pharm Pharmacol*. 2012;6:2346-2353. doi:10.5897/ajpp12.927
18. Gupta M, Singh A, Joshi HC. *Berberis lycium* multipotential medicinal application: an overview. *Int J Chem Stud*. 2015;3:10-13.
19. Ahmad L, Ullah F, Semotiuk AJ, et al. Traditional knowledge and economic significance of *Berberis lycium* Royle in the Lower Dir District, Pakistan. *Ethnobot Res Appl*. 2020;20:1-12.
20. Kapoor B, Sood P, Modgil R, Sood M. *Berberis lycium* a medicinal plant with immense value. *Indian J Pharm Biol Res*. 2013;1:27-37.
21. Ahsan Elahi Bukhari S, Mubashar Sabir S, Ali S, et al. Antioxidant and enzyme inhibitory activities of *Zizypus jujuba*, *Adhatoda vasica* and *Berberis lycium* from hilly areas. *J King Saud Univ Sci*. 2022;34:101980. doi:10.1016/j.jksus.2022.101980
22. Matsuura HN, Fett-Neto AG. Plant alkaloids: main features, toxicity, and mechanisms of action. In: Gopalakrishnakone, P, Carlini, C, Ligabue-Braun, R, eds. *Plant Toxins*. Springer; 2015:1-15.
23. Pereira GC, Branco AF, Matos JA, et al. Mitochondrially targeted effects of berberine [natural yellow 18, 5, 6-dihydro-9, 10-dimethoxybenzo (g)-1, 3-benzodioxolo (5, 6-a) quinolizinium] on K1735-M2 mouse melanoma cells: comparison with direct effects on isolated mitochondrial fractions. *J Pharmacol Exp Ther*. 2007;323:636-649.
24. Malik TA, Kamili AN, Chishti MZ, et al. Breaking the resistance of *Escherichia coli*: antimicrobial activity of *Berberis lycium* Royle. *Microb Pathog*. 2017;102:12-20. doi:10.1016/j.micpath.2016.11.011
25. Shah SAH, Aleem A. Investigations of plausible pharmacodynamics supporting the antispasmodic, bronchodilator, and antidiarrheal activities of *Berberis lycium* Royle. Via in silico, in vitro, and in vivo studies. *J Ethnopharmacol*. 2023;305:116115.
26. Bhalodia NR, Shukla VJ. Antibacterial and antifungal activities from leaf extracts of *Cassia fistula* L.: an ethnomedicinal plant. *J Adv Pharm Technol Res*. 2011;2:104-109.
27. Ali S, Alam M, Khatoon F, et al. Natural products can be used in therapeutic management of COVID-19: probable mechanistic insights. *Biomed Pharmacother*. 2022;147:112658.
28. Piplani S, Singh P, Petrovsky N, Winkler DA. Computational repurposing of drugs and natural products against SARS-CoV-2 main protease (M^{pro}) as potential COVID-19 therapies. *Front Mol Biosci*. 2022;9:781039.
29. Gulfraz M, Fatima N, Parveen Z, Mahmood S. Antimicrobial activity of *Berberis lyceum* Royle against different microorganisms. *Can J Pure Appl Sci*. 2007;1:15-20.

30. Mughal TA, Ali S, Hassan A, et al. Phytochemical screening, antimicrobial activity, in vitro and in vivo antioxidant activity of *Berberis lycium* Royle root bark extract. *Braz J Biol*. 2022;84:e249742.
31. Asif A, Kakub G, Mehmood S, Khunum R, Gulfraz M. Wound healing activity of root extracts of *Berberis lyceum* Royle in rats. *Phytother Res*. 2007;21:589-591.
32. Ali H, Uddin S, Jalal S. Chemistry and biological activities of *Berberis lyceum* Royle. *J Biol Act Prod Nat*. 2015;5:295-312. doi:10.1080/22311866.2015.1073627
33. Shruti A, Agarwal S, Dubey A, Verma A. Evaluation of in vitro anti-inflammatory activity in *Berberis lyceum* Royle of Shivalik range of Himalaya. *Pharma Innov J*. 2021;10:240-243.
34. Manavi MA. In silico study to identification of potential SARS-CoV-2 main protease inhibitors: virtual drug screening and molecular docking with AutoDock Vina and Molegro Virtual Docker. *J Cell Mol Res*. 2022;13:108-112.
35. Al-Ghani R, Nirwani WP, Novianti TN, Sari AGP. In silico anti-inflammatory activity evaluation from *Usnea misaminensis* through molecular docking approach. *Chem Mater*. 2022;1:77-82.
36. Ameji JP, Uzairu A, Shallangwa GA, Uba S. Design, pharmacokinetic profiling, and assessment of kinetic and thermodynamic stability of novel anti-*Salmonella typhi* imidazole analogues. *Bull Natl Res Cent*. 2023;47:6.
37. Šestić TL, Ajduković JJ, Marinović MA, Petri ET, Savić MP. In silico ADMET analysis of the A-, B-and D-modified androstane derivatives with potential anticancer effects. *Steroids*. 2023;189:109147.
38. Lipinski CA, Lombardo F, Dominy BW, Feeney PJ. Experimental and computational approaches to estimate solubility and permeability in drug discovery and development settings. *Adv Drug Deliv Rev*. 2012;64:4-17.
39. Tabrez S, Hoque M, Suhail M, Khan MI, Zughaibi TA, Khan AU. Identification of anticancer bioactive compounds derived from *Ficus* sp. by targeting poly[ADP-ribose]polymerase 1 (PARP-1). *J King Saud Univ Sci*. 2022;34:102079.
40. Afza N, Fatma S, Ghous F, et al. An efficient multicomponent synthesis, characterization, SAR, *In-silico* ADME prediction and molecular docking studies of 2-Amino-7-(substituted-phenyl)-3-cyano-4-phenyl-4, 5, 6, 7-tetrahydropyrano [2, 3-b] pyrrole-5-carboxylic acid derivatives and their in-vitro antimicrobial activity. *J Mol Struct*. 2023;1276:134721.
41. Pourhajibagher M, Bahador A. Virtual screening and computational simulation analysis of antimicrobial photodynamic therapy using propolis-benzofuran A to control of Monkeypox. *Photodiagnosis Photodyn Ther*. 2023;41:103208.
42. Ghose AK, Viswanadhan VN, Wendoloski JJ. A knowledge-based approach in designing combinatorial or medicinal chemistry libraries for drug discovery. *J Comb Chem*. 1999;1:55-68.
43. Veber DF, Johnson SR, Cheng H-Y, Smith BR, Ward KW, Kopple KD. Molecular properties that influence the oral bioavailability of drug candidates. *J Med Chem*. 2002;45:2615-2623.
44. Egan WJ, Merz KM, Baldwin JJ. Prediction of drug absorption using multivariate statistics. *J Med Chem*. 2000;43:3867-3877.
45. Muegge I, Heald SL, Brittelli D. Simple selection criteria for drug-like chemical matter. *J Med Chem*. 2001;44:1841-1846.
46. Omidkhah N, Hadizadeh F, Zarghi A, Ghodsi R. Synthesis, cytotoxicity, Pan-HDAC inhibitory activity and docking study of new N-(2-aminophenyl)-2-methylquinoline-4-carboxamide and (E)-N-(2-aminophenyl)-2-styrylquinoline-4-carboxamide derivatives as anticancer agents. *Med Chem Res*. 2024;32:506-524.
47. Mukhtar M, Khan HA, Zaidi NUSS. Exploring the inhibitory potential of *Nigella sativa* against dengue virus NS2B/NS3 protease and NS5 polymerase using computational approaches. *RSC Adv*. 2023;13:18306-18322. doi:10.1039/d3ra02613b
48. Ayob AZ, Ramasamy TS. Cancer stem cells as key drivers of tumour progression. *J Biomed Sci*. 2018;25:1-18.
49. Asgaonkar K, Tanksali S, Abhang K, Sagar A. Development of optimized pyrimido-thiazole scaffold derivatives as anticancer and multitargeting tyrosine kinase inhibitors using computational studies. *J Indian Chem Soc*. 2023;100:100803.
50. Barazorda-Ccahuana HL Jr, Galvez Ranilla L Jr, Candia-Puma MA Jr, et al. PeruNPDB: the Peruvian Natural Products Database for in silico drug screening. *Sci Rep*. 2023;13:7577.
51. Nagu P, Pathan AKA, Mehta V. Screening of herbal molecules for the management of Alzheimer's disorder through molecular docking and in-vitro investigation. *bioRxiv*. Published online January 2, 2023. doi:10.1101/2023.01.01.522412
52. Gani MA, Nurhan AD, Hadinar Putri BRK, et al. Computational approach in searching for dual action multitarget inhibitors for osteosarcoma. *J Adv Pharm Technol Res*. 2023;14:18-23.
53. Pettersen EF, Goddard TD, Huang CC, et al. UCSF ChimeraX: structure visualization for researchers, educators, and developers. *Protein Sci*. 2021;30:70-82.
54. Goddard TD, Huang CC, Meng EC, et al. UCSF ChimeraX: meeting modern challenges in visualization and analysis. *Protein Sci*. 2018;27:14-25.
55. Biovia Discovery Studio. Discovery Studio 2020. Published 2020. https://discover.3ds.com/discovery-studio-visualizer-download
56. Van Der Spoel D, Lindahl E, Hess B, Groenhof G, Mark AE, Berendsen HJ. GROMACS: fast, flexible, and free. *J Comput Chem*. 2005;26:1701-1718.
57. Jo S, Kim T, Iyer VG, Im W. CHARMM-GUI: a web-based graphical user interface for CHARMM. *J Comput Chem*. 2008;29:1859-1865.
58. Michaud-Agrawal N, Denning EJ, Woolf TB, Beckstein O. MDAnalysis: a toolkit for the analysis of molecular dynamics simulations. *J Comput Chem*. 2011;32:2319-2327.
59. Nakamura T, Isoda N, Sakoda Y, Harashima H. Strategies for fighting pandemic virus infections: integration of virology and drug delivery. *J Control Release*. 2022;343:361-378.
60. Paul A, Chakraborty N, Sarkar A, et al. Ethnopharmacological potential of phytochemicals and phytogenic products against human RNA viral diseases as preventive therapeutics. *Biomed Res Int*. 2023;2023:1977602.
61. Shimu MSS, Mahmud S, Tallei TE, et al. Phytochemical compound screening to identify novel small molecules against dengue virus: a docking and dynamics study. *Molecules*. 2022;27:653. doi:10.3390/molecules27030653
62. Sofowora A, Ogunbodede E, Onayade A. The role and place of medicinal plants in the strategies for disease prevention. *Afr J Tradit Complement Altern Med*. 2013;10:210-229.
63. Chakraborty N, Banerjee A, Sarkar A, Ghosh S, Acharya K. Mushroom polysaccharides: a potent immune-modulator. *Biointerface Res Appl Chem*. 2021;11:8915-8930.
64. Anjum N, Ridwan Q, Akhter F, Hanief M. Phytochemistry and therapeutic potential of *Berberis lycium* Royle; an endangered species of Himalayan region. *Acta Ecol Sin*. 2022;43:577-584. doi:10.1016/j.chnaes.2022.09.005
65. Parra SA, Gaur K, Ranawat LS, Rather MI. An overview on various aspects of plant *Berberis lycium* Royale. *Am J Pharmacol Sci*. 2018;6:19-24.
66. Katare AK, Singh B, Shukla P, et al. Rapid determination and optimisation of berberine from Himalayan *Berberis lycium* by soxhlet apparatus using CCD-RSM and its quality control as a potential candidate for COVID-19. *Nat Prod Res*. 2022;36:868-873.
67. Ilieva Y, Kokanova-Nedialkova Z, Nedialkov P, Momekov G. In silico ADME and drug-likeness evaluation of a series of cytotoxic polyprenylated acylphloroglucinols, isolated from *Hypericum annulatum* Morris subsp. *annulatum*. *Bulg Chem Commun*. 2018;50:193-199.
68. Chandran K, Shane DI, Zochedh A, Sultan AB, Kathiresan T. Docking simulation and ADMET prediction based investigation on the phytochemical constituents of Noni (*Morinda citrifolia*) fruit as a potential anticancer drug. *In Silico Pharmacol*. 2022;10:14.
69. Udugade S, Doijad R, Udugade B. In silico evaluation of pharmacokinetics, drug-likeness and medicinal chemistry friendliness of momordicin1: an active chemical constituent of *Momordica charantia*. *J Adv Sci Res*. 2019;10:222-229.
70. Sarkar P, Srivastava V, Ailani K. Molecular docking simulation, drug pharmacokinetics and synthesis of carbon nanodots from phytochemicals against isoenzymes of cancer. *Mater Today Proc*. 2023;76:289-302.
71. Bouachrine M, Elmchichi L, El Aissouq A, et al. Molecular docking, drug likeness studies and ADMET prediction of flavonoids as platelet-activating factor (PAF) receptor binding. *Chem Rev Lett*. 2021;4:145-152.
72. Mahmud S, Paul GK, Biswas S, et al. Phytochemdb: a platform for virtual screening and computer-aided drug designing. *Database*. 2022;2022:baac002.
73. Preman G, Mulani M, Bare A, et al. Virtual screening of phytochemicals for antitubercular potential using molecular docking approach. *J Tuberc*. 2022;5:1030.
74. Rahmadani K, Manguntungi B, Arwansyah A, et al. Efficiency of nitrification inhibitor on designing nitrogen fertilizer by neem compounds based on molecular docking. *Trends Sci*. 2023;20:6395-6395.
75. Günay MG, Kemerli U, Karaman C, Karaman O, Güngör A, Karimi-Maleh H. Review of functionalized nano porous membranes for desalination and water purification: MD simulations perspective. *Environ Res*. 2023;217:114785.
76. Tripathi N, Bandyopadhyay A. Virtual screening of knottin and defensin peptides perceives hits against the SARS CoV-2 RBD domain and hACE2 interaction. *ChemRxiv*. Published online January 18, 2023. doi:10.26434/chemrxiv-2023-5p74j
77. Gowers RJ, Linke M, Barnoud J, et al. MDAnalysis: a Python package for the rapid analysis of molecular dynamics simulations. Paper presented at: Scipy; July 11, 2016:105; Austin, TX. https://www.osti.gov/servlets/purl/1565806.
78. Tope Abraham I, Ayodele Ifeoluwa F, Peace Ifeoma O, et al. Ethnomedicine claim directed in-silico prediction of epidermal growth factor receptor kinase antagonist: an untapped reservoir of prospective anticancer agents. *World J Adv Res Rev*. 2023;17:662-669. doi:10.30574/wjarr.2023.17.1.0088
79. Al-Khafaji K, Taskin Tok T. Molecular dynamics simulation, free energy landscape and binding free energy computations in exploration the anti-invasive activity of amygdalin against metastasis. *Comput Methods Programs Biomed*. 2020;195:105660.
80. Śledź P, Caflisch A. Protein structure-based drug design: from docking to molecular dynamics. *Curr Opin Struct Biol*. 2018;48:93-102.
81. Ibrahim MA, Abdeljawaad KA, Roshdy E, et al. In silico drug discovery of SIRT2 inhibitors from natural source as anticancer agents. *Sci Rep*. 2023;13:2146.
82. Pande M, Kundu D, Srivastava R. Selective vitamins as potential options for dietary therapeutic interventions: in silico and in vitro insights from mutant C terminal fragment of FGA. *J Steroid Biochem Mol Biol*. 2023;230:106290.
83. Lee Y, Lazim R, Macalino SJY, Choi S. Importance of protein dynamics in the structure-based drug discovery of class AG protein-coupled receptors (GPCRs). *Curr Opin Struct Biol*. 2019;55:147-153.